

De-arbitraging With a Weak Smile: Application to Skew Risk

Babak Mahdavi Damghani

Risk Methodology, SRM, Credit Suisse, e-mail: bmd@cantab.net

Andrew Kos

Risk Methodology, SRM, Credit Suisse

Abstract

The aim of this article is to address the methodology behind de-arbitraging a realistic volatility surface and stressing it without adding arbitrages. We derive from basic principles the constraints which the changes on the strike and the tenor axis must satisfy in order to make a volatility surface arbitrage-free. The two most influential parameterized versions of the volatility surface will then be discussed, along with their origin and their limitations. Furthermore, this review will address the issues of finding the closest arbitrage-free volatility surface through the gSVI method, a more realistic parameterized version of the volatility surface applicable to the FX, commodities, and equities markets. Finally, using examples, the methodology behind coherently stressing this arbitrage-free volatility surface will be looked at, in order to capture and isolate the risk associated with higher-order Greeks like the Vanna or the Vomma.

Keywords

arbitrage-free volatility surface, Dupire local volatility, Fokker-Planck equation, Kolmogorov forward equation, constraint optimization, search algorithm, butterfly spread, calendar spread, arbitrage frontier, SVI, gSVI, skew risk, Vanna, variance reduction technique

1 Introduction

1.1 Scope

Within the framework of options risk modeling, it is essential to define a volatility surface that works with a variety of pricing models. As it happens, most pricing systems used in practice are designed in such a way that they cannot accommodate volatility surfaces that would allow for arbitrage opportunities. In order to address this issue we need to create a methodology that would, first, test whether a volatility surface is arbitrage-free and second, adjust the volatility surfaces that would allow for arbitrages.

The views expressed in this article are the authors' personal views, and unless specifically stated are not those of Credit Suisse.

1.2 Structure of the article

In Section 2 we will explore the condition for an arbitrage-free volatility surface. More specifically, we will show where these conditions come from and we will address an alternative practical form for these conditions. In Section 3 we will make a literature review of the two most influential volatility surface parameterization models, and address their origins and their limitations. We will also introduce the gSVI model in order to address these limitations. We will finally suggest a de-arbitraging methodology in Section 4, and an example application for the skew risk.

2 Derivation of the conditions for arbitrage-free volatility surfaces

2.1 Model setup

The model setup is the usual. Let us set up the probability space $(\Omega, (f)_{(t \geq 0)}, \mathbb{Q})$, with $(f)_{(t \geq 0)}$ generated by the $(T + 1)$ -dimensional Brownian motion and \mathbb{Q} the risk-neutral probability measure under which the discounted price of the underlier, rS , is a martingale. We also assume that the underlier can be represented as a stochastic volatility lognormal Brownian motion as represented by 1. In order to prevent arbitrages on the volatility surface, we will start from basic principles and derive the constraints relevant to the strike and tenor:

$$dS_t = rS_t dt + \sigma_t S_t dW_t \quad (1)$$

2.2 Condition on the strike

2.2.1 Theoretical form

Using Dupire's work [4, 5], we can write the price of a call in the following way:

$$\begin{aligned} C(S_0, K, T) &= e^{-rT} \mathbb{E}^{\mathbb{Q}} [S_T - K]^+ \\ &= e^{-rT} \int_k^{+\infty} (S_T - K) \phi(S_T, T) dS_T \end{aligned} \quad (2)$$

with $\phi(S_T, T)$ being the final probability density of the call. Differentiating twice, we find

$$\frac{\partial^2 C}{\partial K^2} = \phi(S_T, T) > 0 \quad (3)$$

Proof

$$\begin{aligned} C(S_0, K, T) &= e^{-rT} \mathbb{E}^{\mathbb{Q}}[S_T - K]^+ \\ &= e^{-rT} \int_k^{+\infty} (S_T - K) \phi(S_T, T) dS_T \\ \frac{\partial C}{\partial K} &= -e^{-rT} \int_k^{+\infty} \phi(S_T, T) dS_T \\ &= -e^{-rT} \mathbb{E}(S_T > K) \end{aligned}$$

Also, we know that $0 \leq -e^{-rT} \frac{\partial C}{\partial K} \leq 1$. Differentiating a second time and setting $r = 0$, we find $\phi(S_T, T) = \frac{\partial^2 C}{\partial K^2}$. \square

Using numerical approximation we get equation (4), which is known in the industry as the arbitrage constraint of the positivity of the butterfly spread [19]:

$$\boxed{\forall \Delta, C(K - \Delta) - 2C(K) + C(K + \Delta) > 0} \quad (4)$$

Proof

Given that the probability density must be positive, we have $\frac{\partial^2 C}{\partial K^2} \geq 0$. Using numerical approximation, we get

$$\begin{aligned} \frac{\partial^2 C}{\partial K^2} &= \lim_{\Delta \rightarrow 0} \frac{[C(K - \Delta) - C(K)] - [C(K) - C(K + \Delta)]}{\Delta^2} \\ &= \lim_{\Delta \rightarrow 0} \frac{C(K - \Delta) - 2C(K) + C(K + \Delta)}{\Delta^2} \end{aligned}$$

therefore $C(K - \Delta) - 2C(K) + C(K + \Delta) \geq 0$. \square

Gatheral and Jacquier [10] proved that the positivity of the butterfly condition comes back to making sure that the function $g(\cdot)$ from equation (5) is strictly positive:

$$g(k) := \left(1 - \frac{Kw'(k)}{2w(k)}\right)^2 - \frac{w'(k)^2}{4} \left(\frac{1}{w(k)} + \frac{1}{4} + \frac{w''(k)}{2}\right) \quad (5)$$

Proof

We have shown in equation (3) that $\frac{\partial^2 C}{\partial K^2} = \phi(\cdot)$. Applying this formula to the Black-Scholes equation gives, for a given tenor,

$$\phi(k) = \frac{g(k)}{\sqrt{2\pi w(k)}} \exp\left(-\frac{d_2(k)^2}{2}\right) \quad (6)$$

where $w(k, t) = \sigma_{BS}^2(k, t)t$ is the implied volatility at strike K and where $d_2(k) := \frac{-k}{\sqrt{w(k)}} - \sqrt{w(k)}$. \square

Function (5) yields a polynomial of the second degree with a negative highest order, which suggests that the function is inverse bell curve-like and potentially only positive given **two constraints** which may appear as contradicting some of the initial slides Gatheral presented back in 2004. If g_1^e and g_2^e happen to be the exact roots of $g(k) = 0$ with $g_2^e \geq g_1^e$, then the volatility surface is arbitrage-free with respect to the butterfly constraint if $w(k) \leq g_2^e$ and $w(k) \geq g_1^e$.

2.2.2 Practical form

There exists another version of this butterfly [equation (3)] condition that is a necessary but **not sufficient** condition to make a volatility surface arbitrage-free but

remains useful when one has a more practical objective, which will be illustrated with an example in Section 3.4. This condition is given by

$$\boxed{\forall K, \forall T, |T \partial_K \sigma^2(K, T)| \leq 4} \quad (7)$$

Proof

The intuition behind the proof is taken from Rogers and Tehranchi [17], but is somewhat simplified for practitioners. Assuming $r = 0$, let us define the Black-Scholes call function $f: \mathbb{R} \times [0, \infty) \rightarrow [0, 1)$ in terms of the tail of the standard Gaussian distribution $\Phi(x) = \frac{1}{\sqrt{2\pi}} \int_x^{+\infty} \exp(-\frac{y^2}{2}) dy$ and given by

$$f(k, v) = \begin{cases} \Phi\left(\frac{k}{\sqrt{v}} - \frac{\sqrt{v}}{2}\right) - e^k \Phi\left(\frac{k}{\sqrt{v}} + \frac{\sqrt{v}}{2}\right) & \text{if } v > 0 \\ (1 + e^k)^+ & \text{if } v = 0 \end{cases}$$

Let us call $V_t(k, \tau)$ the implied variance at time $t \geq 0$ for log-moneyness k and time to maturity $\tau \geq 0$. Let us now label our Kappa and Vega, with the convention that $\phi(x) = \frac{1}{\sqrt{2\pi}} \exp(-\frac{x^2}{2})$:

$$f_k(k, v) = -e^k \Phi\left(\frac{k}{\sqrt{v}} + \frac{\sqrt{v}}{2}\right)$$

$$f_v(k, v) = \phi\left(\frac{k}{\sqrt{v}} + \frac{\sqrt{v}}{2}\right) / 2\sqrt{v}$$

Now define the function $I: \{(k, c) \in \mathbb{R} \times [0, \infty): (1 + e^k)^+ \leq c < 1\} \rightarrow [0, 1)$ implicitly by the formula

$$f(k, I(k, c)) = c$$

Calculus gives $I_c = \frac{1}{f_v}$ and $I_k = -\frac{f_k}{f_v}$, from here using the chain rule, designating $\partial_{k+} V$ as the right derivative. We have

$$\partial_{k+} V = I_k + I_c \partial_k \mathbb{E}[(S_T - e^k)^+]$$

$$\begin{aligned} \partial_{k+} V &= -\frac{f_k}{f_v} - \frac{\mathbb{P}(S_T > e^k)}{f_v} \\ &< -\frac{f_k}{f_v} = 2\sqrt{v} \frac{\Phi\left(\frac{k}{\sqrt{v}} + \frac{\sqrt{v}}{2}\right)}{\phi\left(\frac{k}{\sqrt{v}} + \frac{\sqrt{v}}{2}\right)} \end{aligned}$$

Now, using the bounds of the Mills ratio $0 \leq 1 - \frac{x\Phi(x)}{\phi(x)} \equiv \varepsilon(x) \leq \frac{1}{1+x^2}$, we have

$$\partial_{k+} V \leq \frac{4}{k/V + 1} < 4$$

Similarly, we can show [17] that $\partial_{k-} V > -4$, therefore we have $|\partial_k V| < 4$. \square

One can think of the boundaries of the volatility surface, as extrapolated by equation (7), as more relaxed boundaries (but still “close”) in the strike space compared with the exact solution from equation (5) set to 0, which are both necessary and sufficient conditions for the volatility surface to be arbitrage-free for the butterfly condition. Formally, if g_1^a and g_2^a happen to be the exact roots of $|T \partial_K \sigma^2(K, T)| - 4 = 0$, with $g_2^a \geq g_1^a$, then we have $g_1^e \leq g_1^a \leq w(k) \leq g_2^a \leq g_2^e$. The reason why equation (7) is practical is because in de-arbitraging methodologies (as we will see in more detail in Section 3.4), there exist for the pricers a component of tolerance anyways (the pricers are stable if the volatility surface is slightly away from its arbitrage frontier). This suggests that finding a close enough solution but building on top of that an iterative

methodology to get closer and closer to the practical arbitrage frontier is almost equally fast, but with less computing trouble, than having the exact theoretical solution (and building an error tolerance finder on top of it anyways). This is because there is less probability of making a typographical error in keying the exact solution of equation (5) (or its numerical approximation), especially if your parameterized version of the volatility surface is complex which is the case for most banks ($\{g_1^a, g_2^a\}$ are easier to find than $\{g_1^e, g_2^e\}$).

2.3 Condition on the tenor

2.3.1 Theoretical form

The condition on the tenor axis which insures the volatility surface to be arbitrage-free is that the calendar spread should be positive:

$$\boxed{C(K, T + \Delta) - C(Ke^{-r\Delta}, T) \geq 0} \quad (8)$$

Proof

One application of Dupire's formula [4, 5] is that the pseudo-probability density must satisfy the Fokker-Planck [7, 16] equation. This proof is taken from El Karoui [13]. Let us apply Itô to the semi-martingale. This is formally done by introducing the local time Λ_u^K :

$$\begin{aligned} & e^{-r(T+\varepsilon)} (S_{T+\varepsilon} - K)^+ - e^{-rT} (S_T - K)^+ \\ &= \int_T^{T+\varepsilon} re^{-ru} (S_u - K)^+ du + \int_T^{T+\varepsilon} e^{-ru} \mathbf{1}_{\{S_u \geq K\}} dS_u \\ &+ \frac{1}{2} \int_T^{T+\varepsilon} e^{-ru} d\Lambda_u^K \end{aligned}$$

Local times are introduced in mathematics when the integrand is not smooth enough. Here the call price is not smooth enough around the strike level at expiry. Now we have $E(e^{-ru} \mathbf{1}_{\{S_u \geq K\}} S_u) = C(u, K) + Ke^{-ru} P(S_u \geq K) = C(u, K) - K \frac{\partial C}{\partial K}(u, K)$. The term of the form $E\left(\int_T^{T+\varepsilon} e^{-ru} d\Lambda_u^K\right)$ is found due to the formula for local times, that is

$$\begin{aligned} E\left(\int_T^{T+\varepsilon} e^{-ru} d\Lambda_u^K\right) &= \int_T^{T+\varepsilon} e^{-ru} du E(\Lambda_u^K) \\ &= \int_T^{T+\varepsilon} e^{-ru} du \sigma^2(u, K) K^2 \phi(u, K) \\ &= \int_T^{T+\varepsilon} \sigma^2(u, K) K^2 \frac{\partial^2 C}{\partial K^2}(u, K) du \end{aligned}$$

Plugging these results back into the first equation, we get

$$\begin{aligned} C(T + \varepsilon, K) &= C(T, K) - \int_T^{T+\varepsilon} rC(u, K) du \\ &+ (r - q) \int_T^{T+\varepsilon} \left(C(u, K) - K \frac{\partial C}{\partial K}(u, K)\right) du \\ &+ \frac{1}{2} \int_T^{T+\varepsilon} \sigma^2(u, K) K^2 \frac{\partial^2 C}{\partial K^2}(u, K) du \end{aligned}$$

If we want to give a PDE point of view of this problem, we can notice that $\phi(T, K) = e^{-rT} \frac{\partial^2 C}{\partial K^2}(T, K)$ verifies the dual forward equation

$$\begin{aligned} \phi'_T(T, K) &= \frac{1}{2} \frac{\partial^2 (\sigma^2(T, K) K^2 \phi(T, K))}{\partial K^2} \\ &- \frac{\partial^2 ((r - q) K \phi(T, K))}{\partial K} \end{aligned}$$

Integrating twice by parts, we find

$$\begin{aligned} \frac{\partial e^{-rT} C(T, K)}{\partial T} &= \frac{1}{2} \sigma^2(T, K) K^2 e^{rT} \frac{\partial^2 C(T, K)}{\partial K^2} \\ &- \int_K^{+\infty} (r - q) Ke^{rT} \frac{\partial^2 C(u, K)}{\partial K^2} \partial K(T, K) du \end{aligned}$$

Now, integrating by parts again and setting dividends to 0, we find the generally admitted relationship

$$\frac{\partial C}{\partial t} = \frac{\sigma^2}{2} K^2 \frac{\partial^2 C}{\partial K^2} - rK \frac{\partial C}{\partial K}$$

and therefore we have

$$\sigma = \sqrt{2 \frac{\frac{\partial C}{\partial t} + rK \frac{\partial C}{\partial K}}{K^2 \frac{\partial^2 C}{\partial K^2}}}$$

From this formula and from the positivity constraint on equation (3), we find that

$$\frac{\partial C}{\partial t} + rK \frac{\partial C}{\partial K} \geq 0$$

Note that for very small Δ :

$$C(Ke^{-r\Delta}, T) \approx C(K - Kr\Delta, T)$$

Using the Taylor expansion:

$$C(K - Kr\Delta, T) = C(K, T) - Kr\Delta \frac{\partial C}{\partial K} + \dots$$

Therefore,

$$rK \frac{\partial C}{\partial K} \approx \frac{C(K, T) - C(Ke^{-r\Delta}, T)}{\Delta}$$

Using forward difference approximation we also have

$$\frac{\partial C}{\partial K} = \frac{C(K, T + \Delta) - C(K, T)}{\Delta}$$

and from Fokker-Planck we have $\frac{\partial C}{\partial t} + rK \frac{\partial C}{\partial K} \geq 0$. Substituting, we obtain

$$\frac{C(K, T + \Delta) - C(K, T)}{\Delta} + \frac{C(K, T) - C(Ke^{-r\Delta}, T)}{\Delta} \geq 0$$

Simplifying, we find $C(K, T + \Delta) - C(Ke^{-r\Delta}, T) \geq 0$. \square

2.3.2 Practical form

Similarly to Section 2.2, there exists a more practical equivalent to the calendar spread criterion. This equivalent criterion is known as the falling variance criterion, which states that:

$$\begin{aligned} &\text{if } S \text{ is a martingale under the risk neutral probability measure } \mathbb{Q}, \\ &\forall t > s, e^{-rt} \mathbb{E}^{\mathbb{Q}}(S_t - K)^+ \geq e^{-st} \mathbb{E}^{\mathbb{Q}}(S_s - K)^+ \end{aligned} \quad (9)$$

Proof

$e^{-rt} \mathbb{E}^{\mathbb{Q}}(S_t - K)^+ \geq e^{-rs} \mathbb{E}^{\mathbb{Q}}(S_s - K)^+ \Rightarrow e^{-rt} \mathbb{E}^{\mathbb{Q}}(S_t - K)^+ - e^{-rs} \mathbb{E}^{\mathbb{Q}}(S_s - K)^+ \geq 0 \Rightarrow$ calendar spread $\geq 0 \Rightarrow C(K, T + \Delta) - C(Ke^{-r\Delta}, T) \geq 0$. \square

3 Parameterizing the volatility surface

3.1 Literature review

If one turns a volatility surface onto a grid, one can check if each point of the grid has an arbitrage using equations (4) and (8). Once the arbitrage points have been detected, we need to move these specific incoherent implied volatility points such that the closest arbitrage-free point is reached. One of the consequences of moving these implied volatilities is that they can create arbitrages in other places of the volatility surface; we therefore need to rerun that “on the fly fixer algorithm” from scratch every time an adjustment has occurred. It seems Lagnado and Osher [14], Crepey [2], and other authors have proposed a minimization algorithm. However, it seems that the financial mathematics literature has not yet reached a consensus on de-arbitraging the volatility surface point by point. With this in mind, the finance industry has developed parameterized versions of the volatility surface because there exist methodologies which allow one to check whether a volatility surface is arbitrage-free via its parameters, a critical point when it comes to utilizing constraints optimization search algorithms. We will explore Schonbucher’s model and the SVI models, which are the last two most influential models of volatility surface parameterization. We will address their limitations and propose an improvement via the gSVI method developed later in this article.

3.2 Schonbucher’s model

In 1999, Schonbucher [18] introduced his parameterized version of the volatility surface. The main advantage of Schonbucher’s model is that it can be derived from the Heston [12] model, which is an underlying model used by many financial institutions and is therefore well respected. He asserts that the implied volatility surface should be modeled through equation (10). Here, x denotes the log-moneyness:

$$I^2(x) = a + bx + \sqrt{\frac{1}{4}\sigma^4 + x^2\nu^2} \quad (10)$$

Proof

Let us define the following Heston [12] model given by the implied volatility I and the stock price S :

$$\begin{cases} dS_t &= rS_t dt + \sigma_t S_t dW_t \\ d\sigma_{k,t} &= u_t dt + \gamma_t dW_t + \nu_t dW_t^\perp \\ \gamma_t^2 + \nu_t^2 &= 1 \end{cases}$$

The two Brownian motions are independent of each other.¹ The implied stock volatility function $\sigma_{k,t}$ is yet to be specified; to simplify the notation, let us redefine this variable as I_t and call γ_t the correlation between the instantaneous volatility and the spot price, with ν_t chosen such that $\gamma_t^2 + \nu_t^2 = 1$. Now, apply Itô’s lemma to the call price to obtain the drift restriction

$$\begin{aligned} rC^{BS} &= \frac{\partial C^{BS}}{\partial t} + rS \frac{\partial C^{BS}}{\partial S} + u \frac{\partial C^{BS}}{\partial I} \\ &+ \gamma \sigma S \frac{\partial^2 C^{BS}}{\partial I \partial S} + \frac{1}{2} (\sigma^2 S^2 \frac{\partial^2 C^{BS}}{\partial S^2} + \frac{\partial^2 C^{BS}}{\partial I^2}) \end{aligned}$$

Using the Black–Scholes formula for the call and its derivatives, this reduces to a joint restriction on the implied and instantaneous volatility:

$$Iu = \frac{1}{2(T-t)}(I^2 - \sigma^2) - \frac{1}{2}d_1 d_2 \nu^2 + \frac{d_2}{\sqrt{T-t}} \sigma \gamma \quad (11)$$

where we have used the standard definitions for d_1 and d_2 :

$$\begin{aligned} d_1 &= \frac{x}{I\sqrt{T-t}} + \frac{1}{2}I\sqrt{T-t} \\ d_2 &= d_1 - I\sqrt{T-t} \end{aligned}$$

Equation (11) blows up as $T - t$ goes to zero. This imposes the condition that

$$(I^2 - \sigma^2) - d_1 d_2 \nu^2 (T - t) + d_2 \sigma \gamma \sqrt{T - t} = O(T - t)$$

and thus in the limit, noting that $\lim_{t \rightarrow T} d_1 \sqrt{T - t} = \lim_{t \rightarrow T} d_2 \sqrt{T - t} = \frac{1}{I} \ln\left(\frac{S}{K}\right)$ and by setting a zero correlation between spot and implied vol,² the solution becomes

$$I^2(x) = \frac{1}{2}\sigma^2 + \sqrt{\frac{\sigma^4}{4} + x^2\nu^2}$$

Note that there is no ATM skew, but this is easily remedied by adding an extra linear term:

$$I^2(x) = a + bx + \sqrt{\frac{\sigma^4}{4} + x^2\nu^2} \quad \square$$

3.3 The stochastic volatility inspired (SVI) model

Like Schonbucher’s model, the advantage of the SVI is that it can be derived from Heston [9, 12], a model used by many financial institutions and which can therefore be taken as legitimate. However, it did not come with non-arbitrage constraints and its parameters are not as intuitive as they could be for traders. These are the two main contributions of the SVI, developed by Gatheral [8] in 2005 and for which the non-arbitrage-free constraints were clarified in 2012 [10]. For each time to expiry, he writes

$$\sigma_{BS}(k) = a + b[\rho(k - m) + \sqrt{(k - m)^2 + \sigma^2}] \quad (12)$$

where:

- k is the log-moneyness [$\log(\frac{K}{F})$, with S being the value of the forward]
- a adjusts the vertical displacement of the smile
- b adjusts the angle between the left and right asymptotes
- σ adjusts the smoothness of the vertex
- ρ adjusts the orientation of the graph
- m is the horizontal displacement of the smile

The advantage of Gatheral’s model was that it was a parametric model that was easy to use, yet had enough complexity to properly model the volatility surface and its dynamic³ (or at least to the same extent Schonbucher’s model did). Note that Schonbucher’s market model has one parameter less than the SVI: the m parameter, whose aim is to center the volatility surface around its minimum strike per tenor. Other than this, the two models are equivalent.⁴ But at the same time, it was simple enough that a solution could be found using simple optimization by constraint algorithms. Figure 1 illustrates the change in the ρ parameter (the skew risk), Figure 2 illustrates the change in the b parameter (the vol of vol risk), Figure 3 illustrates the

Figure 1: Impact of a change in ρ from 0 to -0.8 in the SVI/gSVI model ($b = 0.35, a = 0.01, \sigma = 0.01$, and $m = 0$ stay constant)

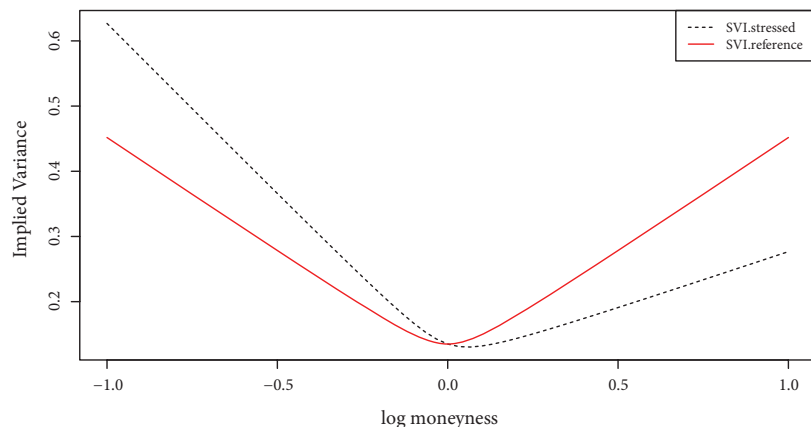


Figure 2: Impact of a change in b from 0.35 to 0.5 in the SVI/gSVI model ($\rho = 0, a = 0.1, \sigma = 0.01$, and $m = 0$ stay constant)

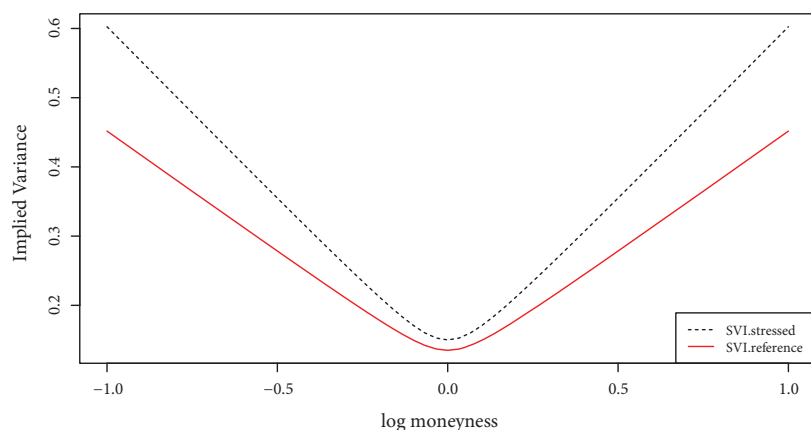
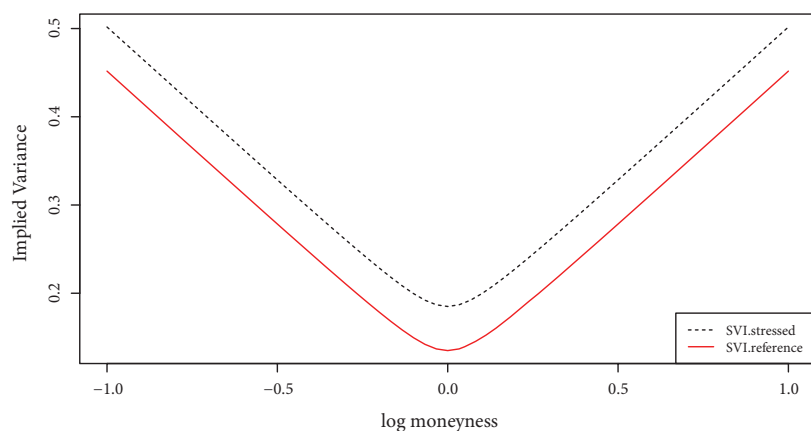


Figure 3: Impact of a change in a from 0.1 to 0.15 in the SVI/gSVI model ($\rho = 0, b = 0.35, \sigma = 0.01$, and $m = 0$ stay constant)



change in the a parameter (the general volatility level risk), Figure 4 illustrates the change in the σ parameter (the ATM volatility risk), and finally Figure 5 illustrates the change in the m parameter (the horizontal displacement risk).

Figure 4: Impact of a change in σ from 0.01 to 0.03 in the SVI/gSVI model ($\rho = 0, b = 0.35, a = 0.1$, and $m = 0$ stay constant)

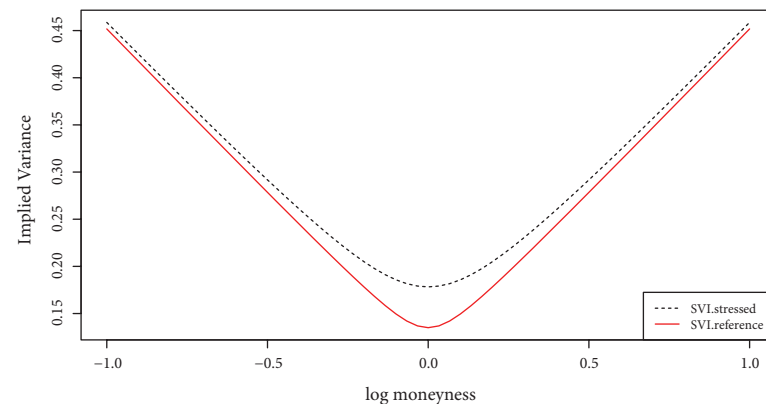
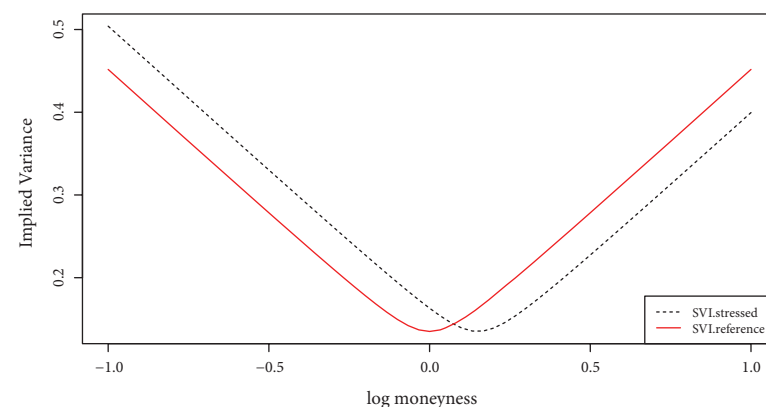


Figure 5: Impact of a change in m from 0 to 0.15 in the SVI/gSVI model ($\rho = 0, b = 0.35, a = 0.1$, and $m = 0$ stay constant)



3.3.1 The SVI's constraints

The SVI has **three** necessary and sufficient conditions which make it arbitrage-free. On top of these three constraints, the SVI has three other constraints that do not reduce the state-space but decrease the probability of falling into a local minimum during the optimization process. We have seen in equation (7) the general condition that makes a volatility surface “often” arbitrage-free along the strike axis. This condition translates to equation (13) for the SVI model:

$$b(1 + |\rho|) \leq \frac{4}{T} \quad (13)$$

Proof

We know that $\forall x, \forall T, |T\partial_x \sigma_{BS}^2(k)| \leq 4$, and we know $\sigma_{BS}(k) = a + b[\rho(k - m) + \sqrt{(k - m)^2 + \sigma^2}]$.

$$|T[b\rho + b \times (k)]| \leq 4$$

$$|T[b(k + \rho)]| \leq 4$$

$$|T[b(1 + \rho)]| \leq 4$$

$$b(1 + |\rho|) \leq \frac{4}{T}$$

□

Note that we have mentioned the volatility surface is *often* arbitrage-free and not *always*. This is because equation (7) is a necessary but not sufficient condition for your volatility surface to be arbitrage-free with respect to the butterfly condition. A counter-example was given by Axel Vogt on wilmott.com. He asserts that with the following SVI parameters: $(a, b, m, \rho, \sigma) = (-0.0410, 0.1331, 0.3586, 0.3060, 0.4153)$, one satisfies equation (13) yet we get a butterfly condition.

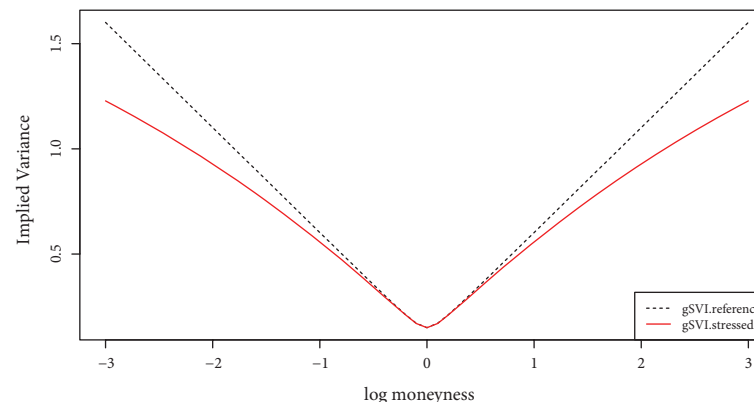
3.4 The generalized stochastic volatility inspired (gSVI) model

Jim Gatheral developed the SVI model at Merrill Lynch in 1999, but it was implemented in 2005. The SVI was subsequently decommissioned in 2010 because of its limitations in accurately pricing out-of-the-money variance swaps (e.g., short-maturity Var swaps on the Eurostoxx are overpriced when using the SVI). This is because the wings of the SVI are linear and have a tendency to overestimate the OTM variance swaps. Benaim *et al.* [1] gave a mathematical justification for this market observation. The paper suggests that the implied volatility cannot grow asymptotically faster than \sqrt{k} but may grow slower than \sqrt{k} when the distribution of the underlier does not have finite moments (e.g., has heavy tails). This suggests that the linear wings of the SVI model may overvalue really deeply OTM options, which is observable in the markets. In order to address the limitations of the SVI model in the wings, we propose a penalization of the wings function. The additional relevant parameter will be called β and aims to address this specific issue. The penalization will be symmetrical in the FX market, more significant on the left wing of the equities market and more significant on the right wing of the commodities (in general, e.g., excluding oil) market due to the smile, skew, and inverse skew features observable on these different markets. The function needs to be increasing as it gets further away from m and majored by a linear function increasing in $[m; +\infty[$ and decreasing in $]-\infty; m]$ and increasing in concavity the further away it gets from the center. The real modeling contribution of the gSVI with respect to the SVI is this penalization change of variable and its corresponding constraints adjustments. Equation (14) summarizes the gSVI model. The penalization will be given by $z = \frac{k-m}{\beta^{|k-m|}}$, which is a function that is strictly increasing between log-moneyness 0 and 3 when $1 \leq \beta \leq 1.4$, similarly decreasing between -3 and 0. There are two main reasons why we have chosen the gSVI model. First, the more parameters a model has, the more flexibility it allows for reproducing subtleties on the volatility surface. However, the more parameters a model has, the harder it is to calibrate it as the risk of falling into local minima increases. This means that the question of model selection is an optimization problem on its own. We believe that the gSVI has enough parameters to accurately model the volatility surface without the risk of falling into the traps of basic search algorithms. Also, the geometrical properties of the gSVI makes it especially attractive when it comes to finding seed parameters for the optimization by constraints algorithm. Figure 1 illustrates the change in the ρ parameter, Figure 2 illustrates the change in the b parameter, Figure 3 illustrates the change in the a parameter, Figure 4 illustrates the change in the σ parameter, Figure 5 illustrates the change in the m parameter, and finally, Figure 6 illustrates the change in the β parameter. The geometric properties of the gSVI, more specifically its ability to model smile, skew, and inverse skew, while at the same time correcting the linear wings of the SVI, makes it applicable to the FX, commodities, and equities markets. The rates markets need another parameterization and an additional dimension, which is beyond the scope of this article.

$$\sigma_{gSVI}^2(k) = a + b \left[\rho(z - m) + \sqrt{(z - m)^2 + \sigma^2} \right]$$

$$z = \frac{k - m}{\beta^{|k - m|}}, 1 \leq \beta \leq 1.4$$
(14)

Figure 6: Impact of a change in β from 1 to 1.1 in the gSVI model ($\rho = 0, b = 0.35, a = 0.1, \sigma = 0.01$, and $m = 0$ stays constant)



There exist two constraints that make gSVI “often” (as explained in Section 3.3.1) arbitrage-free. The first condition on the falling variance [equation (9)] does not change. However, we need to adjust for equation (13), which is replaced in the gSVI by equation (15):

$$\left| T \frac{1 + |k - m| \ln \beta}{\beta^{|k - m|}} \left(b\rho + \frac{\left(\frac{k - m}{\beta^{|k - m|}} - m\right)}{\sqrt{\left(\frac{k - m}{\beta^{|k - m|}} - m\right)^2 + \sigma^2}} \right) \right| \leq 4 \quad (15)$$

Proof

We know that $\partial_k \sigma_{gSVI}^2(k) = \frac{\partial z}{\partial k} \times \frac{\partial \sigma}{\partial z}$. Calculus gives

$$\frac{\partial z}{\partial k} = \frac{1 + (k - m) \ln \beta (1_{k > m} - 1_{k < m})}{\beta^{|k - m|}} = \frac{1 + |k - m| \ln \beta}{\beta^{|k - m|}}$$

$$\frac{\partial \sigma}{\partial z} = b\rho + \frac{2(z - m)}{2\sqrt{(z - m)^2 + \sigma^2}} = b\rho + \frac{\left(\frac{k - m}{\beta^{|k - m|}} - m\right)}{\sqrt{\left(\frac{k - m}{\beta^{|k - m|}} - m\right)^2 + \sigma^2}}$$

Now, plugging in equation (7) the constraint becomes

$$\left| T \frac{1 + |k - m| \ln \beta}{\beta^{|k - m|}} \left(b\rho + \frac{\left(\frac{k - m}{\beta^{|k - m|}} - m\right)}{\sqrt{\left(\frac{k - m}{\beta^{|k - m|}} - m\right)^2 + \sigma^2}} \right) \right| \leq 4$$

□

4 Bumping and “de-arbitraging” the volatility surface

4.1 Bumping the volatility surface

There are many methodologies for bumping the volatility surface. One can either do scenario analysis, for example, if one wants to know what happens if the volatility of a particular point moves by x amount. One might like to know whether the induced volatility surface is arbitrage-free or not and, if not, to what extent one can stress that particular point until an arbitrage has been reached. Similarly, one could be working within a risk department in an investment bank and be asked to investigate what the associated risk is for a certain product. More specifically, one might like to know

the associated risk with respect to the change in volatility only. One could record the proportional historical move of the volatility surface on sticky⁵ log-moneyness and apply these moves to today's volatility surface. One would want to make sure that the induced volatility surface is arbitrage-free. Let us call these various bumped volatility surfaces a target volatility surface σ_{target} .

4.2 De-arbitraging the volatility surface

We would like to insure that σ_{target} is arbitrage-free. The closest arbitrage-free volatility surface will be given by equation (16) subject to constraints (9), (7). For the sake of clarity, let us set $\Omega = \mathbf{U}_{t_1 \leq t \leq T}(\rho, \sigma, a, b, m, \beta)$:

$$\hat{\Omega} = \underbrace{\arg \min}_{\Omega} \sum_{t=t_1}^T \sum_{i=1}^N [\sigma_{gSVI,t}(K_i) - \sigma_{target,t}(K_i)]^2 \quad (16)$$

In order to ease the optimization we have set three additional constraints given by equation (17). Martini [15] suggested the first three constraints, the last one being the trivial constraint:

$$\begin{aligned} \sigma &\geq 0 \\ b &> 0 \\ \rho &\in [-1, 1] \\ \sigma_{gSVI}(K) &> 0 \end{aligned} \quad (17)$$

The complete optimization problem for the "often" de-arbitrager per tenor, t , is given by

$$\begin{aligned} &\text{solve:} \\ &\hat{\Omega} = \underbrace{\arg \min}_{\Omega} \sum_{t=t_1}^T \sum_{i=1}^N [\sigma_{gSVI,t}(K_i) - \sigma_{target,t}(K_i)]^2 \\ &\text{subject to:} \\ &\left| \frac{T}{4} \frac{1 + |k - m| \ln \beta}{\beta^{|k-m|}} \left(b\rho + \frac{\left(\frac{k-m}{\beta^{|k-m|}} - m\right)}{\sqrt{\left(\frac{k-m}{\beta^{|k-m|}} - m\right)^2 + \sigma^2}} \right) \right| \leq 4 \\ &e^{-rt} \mathbb{E}^{\mathbb{Q}}(S_t - K)^+ \geq e^{-rs} \mathbb{E}^{\mathbb{Q}}(S_s - K)^+ \\ &\sigma_t \geq 0 \\ &b_t > 0 \\ &\rho_t \in [-1, 1] \\ &\sigma_{t,gSVI}(K_i) > 0 \end{aligned} \quad (18)$$

4.3 Calibration algorithm and moving away from the arbitrage frontier

Practitioners will be happy to hear that this optimization algorithm can easily be set up with the Excel solver. In order to avoid falling into a local minimum and because the search is multidimensional, it is necessary to help the search algorithm with well-chosen seed parameters. Setting m and a to the observed minimum, σ and β to 0, and ρ and b to the solutions of a system of a couple of linear regressions yields good initial seed parameters. A better seed parameter is found for β by perturbing the initially chosen seed for the b parameter and applying a joint gradient descent on b and β .

On a more practical aspect, note that within the framework of a financial institution,

each product of each market may have its own pricer. Depending on the complexity of the product, the relevant pricer might be more or less sensitive to numerical instabilities and therefore to the volatility surface being close to the arbitrage frontier. Owing to this complication because of these potential error tolerances, the pricer must use a volatility surface slightly away from its arbitrage frontier. It is therefore possible that the algorithm described by equation (18) fails because the calibrated volatility surface is too close to the theoretical arbitrage frontier. In order to address this particular practical issue, we propose the following methodology, which aims to iteratively move away from this theoretical arbitrage frontier. The two critical constraints for the volatility surface are given by equations (15) and (9), corresponding to the constraints of the butterfly and the calendar spread. If one needs to move away from the arbitrage frontier, one needs to adjust these constraints. The methodology will consist of iteratively making these two constraints more and more conservative until the pricer accepts the volatility surface created. With this in mind, if e_1 and e_2 correspond to the degree of conservativeness with respect to the arbitrage frontier for the butterfly and calendar spread constraints, respectively, e_1 and e_2 will initially be set to 0 and then the constraints of equations (15) and (9) are adjusted to equations (19) and (20). Algorithm 1 describes the details of this protocol in pseudo-code:

$$\left| \frac{T}{4} \frac{1 + |k - m| \ln \beta}{\beta^{|k-m|}} \left(b\rho + \frac{\left(\frac{k-m}{\beta^{|k-m|}} - m\right)}{\sqrt{\left(\frac{k-m}{\beta^{|k-m|}} - m\right)^2 + \sigma^2}} \right) \right| \leq e_1 \quad (19)$$

$$\frac{e^{-rt} \mathbb{E}^{\mathbb{Q}}(S_t - K)^+}{e^{-rs} \mathbb{E}^{\mathbb{Q}}(S_s - K)^+} \geq e_2 \quad (20)$$

Algorithm 1

De-arbitrages a practical volatility surface

Require: A volatility surface $\mathbf{U}\sigma(k)$ and an error tolerance tuple e_1, e_2

Ensure: $\mathbf{U}\sigma(k)$ is arbitrage-free in a practical sense

$\mathbf{U}\sigma(k) \leftarrow \text{dearbVol}(\mathbf{U}\sigma(k))$

isError Price($\mathbf{U}\sigma(k)$)

$e_1 = 1, e_2 = 1, \varepsilon_1 > 0, \varepsilon_2 > 0$

while isError gives an error **do**

if butterfly arbitrage **then**

$e_1 \leftarrow e_1 - \varepsilon_1$

 adjust butterfly constraint to $\left| \frac{T}{4} \frac{1 + |k - m| \ln \beta}{\beta^{|k-m|}} \right|$

$$\left(b\rho + \frac{\left(\frac{k-m}{\beta^{|k-m|}} - m\right)}{\sqrt{\left(\frac{k-m}{\beta^{|k-m|}} - m\right)^2 + \sigma^2}} \right) \leq e_1$$

else

$e_2 \leftarrow e_2 - \varepsilon_2$

 adjust calendar constraint to $\frac{e^{-rt} \mathbb{E}^{\mathbb{Q}}(S_t - K)^+}{e^{-rs} \mathbb{E}^{\mathbb{Q}}(S_s - K)^+} \geq e_2$

end if

 dearbVol($\mathbf{U}\sigma(k), e_1, e_2$) as described by equation (18) with the adjustments

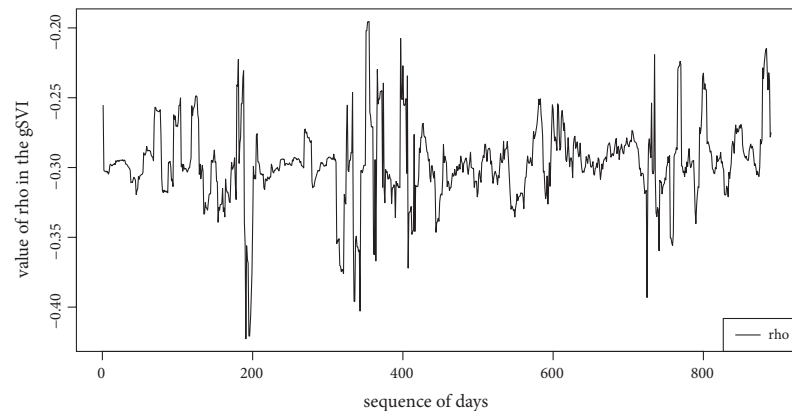
 isError Price($\mathbf{U}\sigma(k)$)

end while

4.4 De-arbitrage example: Skew risk

Let us look at the following case. One has been assigned the task of creating a model that studies skew risk, or more formally, Vanna, $\frac{\partial^2 V}{\partial \sigma \partial S}$.⁶ You notice that the

Figure 7: Evolution of the ρ parameter in the gSVI for the FTSE from 10/02/2011 back 890 days on the tenor with 14 years expiry



ρ parameter gives the dynamics of the skew and decide to plot the evolution of this parameter through time (Figure 7).

4.4.1 Traditional methodology

One assumes that the ρ parameter is independent with respect to the other parameters of the gSVI.⁷ One decides to apply historical bumps to one's ρ parameter and also to apply these to the most recent volatility surface, in order to get a sequence of skew risk P&L strips. Note that when the bumps are applied, a numerical transform function must be applied in order to insure that one's ρ parameter stays within its domain of definition. A Fisher-like transform [6] insures that ρ stays within its domain of definition. However, how realistic this transform is in terms of approximating the realized numerical transform function is yet to be proven. Figure 8 represents a theoretical volatility surface without an arbitrage. Figure 9 represents its stressed version (changing the ρ parameter in the gSVI model) with an arbitrage and Figure 10 represents its closest arbitrage-free volatility surface given by equation (23).⁸

4.4.2 A better, more realistic methodology

The numerical transform function assumes an underlying distribution for the bumps which is inconvenient, because the method may not be transferable to other products and other asset classes if the correct transform function has already been calibrated for a specific product. A simple observation of the historical dynamics of the ρ parameter in Figure 7 suggests that ρ is stationary⁹ and could be represented by a modified Ornstein–Uhlenbeck (OU) [11] process as described by equation (24) (μ is the long-term mean, θ the recall force, and σ_o is the volatility of the stochastic part of the OU process). In equation (24), dD_t represents the dynamic of a random process (e.g., dW_t) that we will estimate empirically. The modification of the OU process (the $\sqrt{1 - \rho_t^2}$ term in front of the stochastic part of the differential equation) is added in order to insure that the ρ parameter stays within its boundary definition $[-1; 1]$.¹⁰ The μ parameter can be estimated by taking the average value of ρ , that is, $\mu = \mathbb{E}[\rho]$.¹¹ By rearranging equation (24) and taking the expectation, we find $\hat{\theta} = \mathbb{E}\left[\frac{d\rho_t}{(\hat{\mu} - \rho_t)dt}\right]$ and $\hat{\sigma}_o = \sqrt{\text{Var}\left[\frac{d\rho_t - \hat{\theta}(\hat{\mu} - \rho_t)dt}{\sqrt{1 - \rho_t^2}dD_t}\right]}$. The issue with this

methodology is that $\hat{\theta}$ converges very slowly and therefore $\hat{\sigma}_o$ does as well. Adding to this issue, the data might literally not be there at all. It is therefore primordial to come up with a variance reduction technique. The inspiration behind the variance

Figure 8: Plot of a fictitious volatility surface without arbitrage

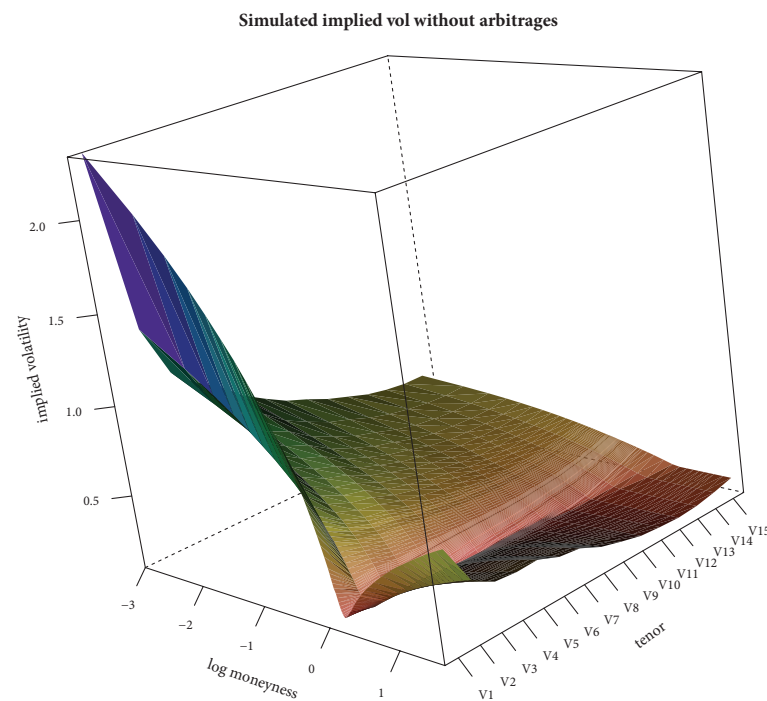
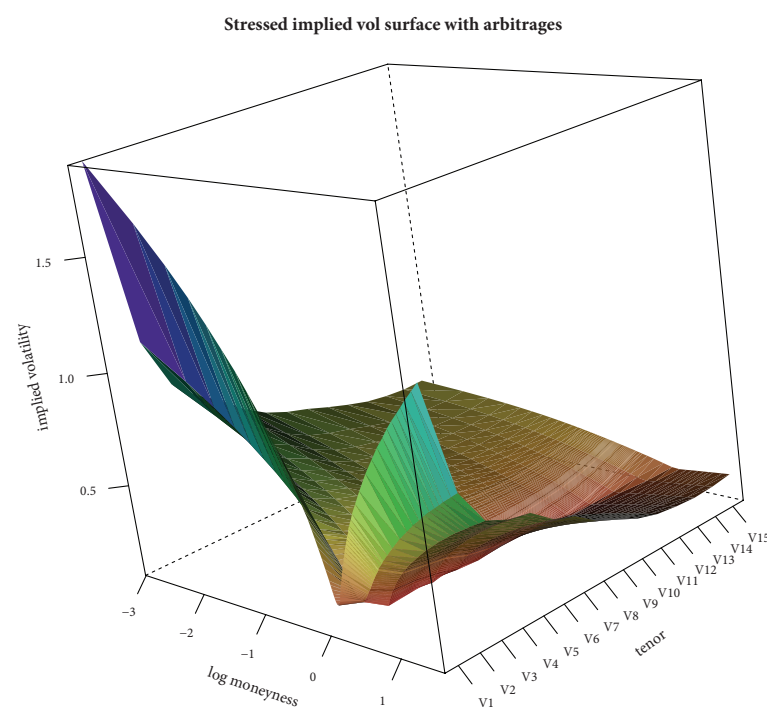
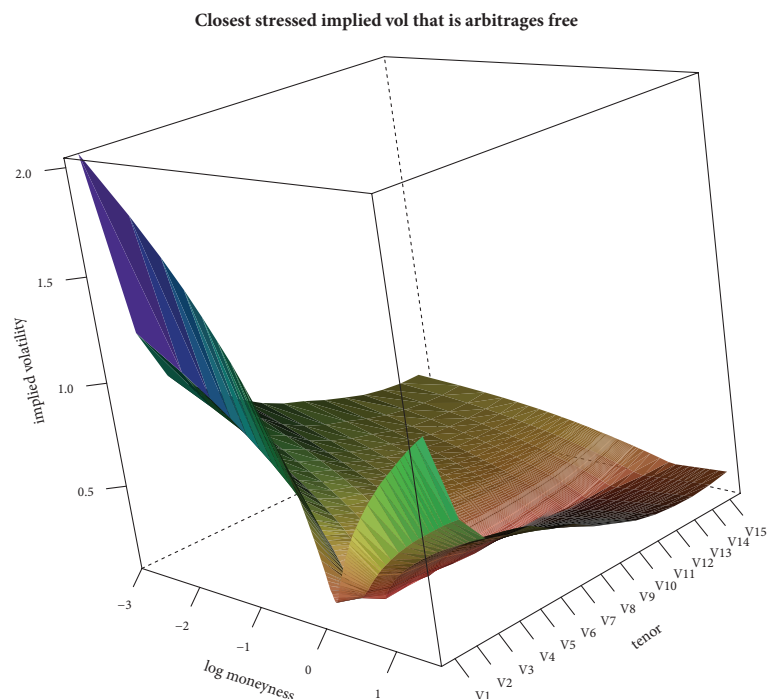


Figure 9: Plot of a stressed version of Figure 8



reduction technique comes from noticing that in equation (24), θ 's estimation is perturbed by the stochastic part of the differential equation, especially intense when ρ_t is close to 0. Similarly, σ_o 's estimation is perturbed when ρ_t^2 is close to 1. The variance

Figure 10: Closest arbitrage-free version of volatility surface from Figure 9, keeping all the parameters constant but ρ



reduction technique will consist of sampling θ either when $\rho_t^2 = 1$ or if this never occurs, only when $\rho_t^2 > B_+$ where $-1 < B_+ < 1$ is defined by equation (25) and is supposed to represent an upper barrier. The variance reduction technique yields equation (26) for θ . Similarly, the variance reduction technique will consist of sampling σ_o either when $\rho_t = \mu$ or if this never occurs, only when $|\rho_t| < B_-$ where $-1 < B_- < 1$ is defined by equation (27) and is supposed to represent a lower barrier. The variance reduction technique yields equation (28) for σ_o .

$$\bigcup_{t_1 \leq t \leq T} \hat{\rho}_t = \arg \min_{\rho_t} \left[\sum_{t=t_1}^T \sum_{i=1}^N \sigma_{gSVI,t}(K_i) - \sigma_{target,t}(K_i) \right]^2 \quad (23)$$

$$d\rho_t = \theta(\mu - \rho_t)dt + \sqrt{1 - \rho_t^2} \sigma_o dD_t \quad (24)$$

$$B_+ = \max\left(\left|\frac{\sup(\rho) + \mu}{2}\right|, \left|\frac{\inf(\rho) + \mu}{2}\right|\right) \quad (25)$$

$$\hat{\theta} = \mathbb{E}\left[\frac{d\rho_t}{(\hat{\mu} - \rho_t)dt} \mathbf{1}_{|\rho_t| > B_+}\right] \quad (26)$$

$$B_- = \min\left(\left|\frac{\sup(\rho) + \mu}{2}\right|, \left|\frac{\inf(\rho) + \mu}{2}\right|\right) \quad (27)$$

$$\hat{\sigma}_o = \sqrt{\text{Var}\left[\frac{d\rho_t - \hat{\theta}(\hat{\mu} - \rho_t)dt}{\sqrt{1 - \rho_t^2}dD_t} \mathbf{1}_{|\rho_t| < B_-}\right]} \quad (28)$$

$$\begin{aligned} d\rho_t &= \theta(\mu - \rho_t)dt + \sqrt{1 - \rho_t^2} \sigma_o dD_t \\ \hat{\mu} &= \mathbb{E}[\rho_t] \\ \hat{\theta} &= \mathbb{E}\left[\frac{d\rho_t}{(\hat{\mu} - \rho_t)dt} \mathbf{1}_{|\rho_t| > B_+}\right] \\ B_+ &= \max\left(\left|\frac{\sup(\rho) + \mu}{2}\right|, \left|\frac{\inf(\rho) + \mu}{2}\right|\right) \\ \hat{\sigma}_o &= \sqrt{\text{Var}\left[\frac{d\rho_t - \hat{\theta}(\hat{\mu} - \rho_t)dt}{\sqrt{1 - \rho_t^2}dD_t} \mathbf{1}_{|\rho_t| < B_-}\right]} \\ B_- &= \min\left(\left|\frac{\sup(\rho) + \mu}{2}\right|, \left|\frac{\inf(\rho) + \mu}{2}\right|\right) \\ \hat{\rho}_t &= \max\left(\min(\rho_{t-1} + \hat{\theta}(\hat{\mu} - \rho_{t-1})dt + \sqrt{1 - \rho_{t-1}^2} \hat{\sigma}_o d\hat{D}_t, 1), -1\right) \\ \bigcup_{t_1 \leq t \leq T} \hat{\rho}_t &= \text{dearb And Return Closest Rho} \\ &\quad \left(\bigcup_{t_1 \leq t \leq T} \bigcup_{1 \leq i \leq N} \sigma_{target,t}(K_i), \bigcup_{t_1 \leq t \leq T} \hat{\rho}_t \right) \end{aligned} \quad (29)$$

5 Conclusion

We showed that the positivity constraint on the butterfly and the calendar spread are the two necessary and sufficient conditions that make a volatility surface arbitrage-free. More specifically, we saw that the butterfly condition can be derived from differentiating twice the call price with respect to the strike. We saw that the calendar spread constraint can be derived from rearranging the Fokker-Planck equation into Dupire's local volatility equation and extracting the calendar spread payoff from the numerator. We then expressed these two constraints into a more user-friendly form for practitioners interested in finding a parameterized version of the volatility surface. This led us to make a literature review of the two most influential parameterized versions of the volatility surface, which are Schonbucher's model and Gatheral's SVI. More specifically, we saw how Schonbucher's model was derived from the Heston model and how SVI improved Schonbucher's model by adding non-arbitrage constraints. We also demonstrated the limitations of this model by introducing the change of variable with the aim of adjusting the wings of the SVI model, an observable and mathematically justifiable limitation of the SVI model. We also described a de-arbitraging methodology for stressed volatility surfaces and, finally, gave an example of the application of a skew risk methodology which uses the de-arbitraging methodology along with a modified OU process.

Babak Mahdavi Damghani has been working in the financial industry within the quantitative space (Exotics Trading, High Frequency Quantitative Analytics and Structuring) since 2007, currently working as a Quantitative Analyst at Credit Suisse. He has done his postgraduate studies in the applied mathematical and computing sciences at the University of Cambridge, at the Ecole Polytechnique in Paris and at the University of Oxford.

Andrew Kos holds a Masters degree in Mathematics from Durham University. He also holds a distinction in the CQF and has qualified as an accountant under the Chartered Institute of Management Accountants.

ENDNOTES

1. W_t^+ is independent of W_t .
2. A simplification made by Schonbucher but not necessarily very realistic, specifically on the commodities market where for physical reasons the stochastic processes driving the commodities are more driven by mean reversion than classic correlation [3].
3. We will see its main limitation when we explore the gSVI.
4. Indeed, in equation (10) replace k by $k - m$, replace b by $b\rho$, and replace $\frac{\sigma^2}{4}$ by $\frac{\sigma^2}{b^2}$ to get equation (12).
5. The log-moneyness in the reference volatility surface does not change, so the strikes are adjusted with respect to the change in spot.
6. If Δ is your delta and if V represents your vega, alternative representations are: $\frac{\partial \Delta}{\partial \sigma}$ or $\frac{\partial V}{\partial \zeta}$.
7. Not necessarily the most realistic assumption, especially with the b parameter.
8. Note that some banks define skew as the slope of the equation tangent to the ATM forward. In this case, the bump will not be applied to the ρ parameter but to

$$\partial_x \sigma^2(k) = \frac{1 + |k - m| \ln \beta}{\beta^{|k-m|}} \times \left(b\rho + \frac{\left(\frac{k-m}{\beta^{|k-m|}} - m\right)}{\sqrt{\left(\frac{k-m}{\beta^{|k-m|}} - m\right)^2 + \sigma^2}} \right), \text{ where } x \text{ is the}$$

log-moneyness. Setting x to the ATM forward ($k = m$), we get equation (21). ζ will denote the skew with this alternative definition.

9. The fact that ρ is bounded insures its stationarity.
10. Assuming the other parameters are independent, we get equation (22) for the dynamics of the skew if the bank definition is chosen.

$$\zeta = b\rho - \frac{m}{m^2 + \sigma^2} \tag{21}$$

$$d\zeta_t = b[\theta(\mu - \rho_t)dt + \sqrt{1 - \rho_t^2} \sigma_o dD_t] - \frac{m}{m^2 + \sigma^2} \tag{22}$$

11. This result can be justified with Doob's forward convergence theorem ($\rho \in [-1, 1]$ therefore bounded).

REFERENCES

[1] S. Benaim, P. Friz, and R. Lee. 2008. On the Black-Scholes implied volatility at extreme strikes. In *Frontiers in Quantitative Finance: Volatility and Credit Risk Modeling* (ed R. Cont), Wiley: Hoboken, NJ. doi: 10.1002/9781118266915.ch2 <http://onlinelibrary.wiley.com/doi/10.1002/9781118266915.ch2/summary>.

[2] S. Crepey. 2003. Calibration of the local volatility in a trinomial tree using Tikhonov regularization. *Institute of Physics Publishing, Inverse Problems* 19, 91–127. <http://iopscience.iop.org/0266-5611/19/1/306/>.

[3] B.M. Damghani, D. Welch, C. O'Malley, and S. Knights. 2012. The misleading value of measured correlation. *Wilmott magazine*, November 64–73.

[4] B. Dupire. 1994. Pricing with a smile. *Risk* January, pp. 17–20. http://www.risk.net/data/risk/pdf/technical/2007/risk20_0707_technical_volatility.pdf.

[5] B. Dupire. 1997. Pricing and hedging with a smile, pp. 103–111. In M.A.H. Dempster and S.R. Pliska (eds), *Mathematics of Derivative Securities*. Isaac Newton Institute. Cambridge University Press: Cambridge, UK.

[6] R.A. Fisher. 1915. Frequency distribution of the values of the correlation coefficient in samples from an indefinitely large population, 10:507–521. Available at: <http://www.jstor.org/stable/2331838>.

[7] A. Fokker. 1914. Die mittlere energie rotierender elektrischer dipole im strahlungsfeld, *Annalen der Physik* 348:5, 810–820. <http://onlinelibrary.wiley.com/doi/10.1002/andp.19143480507/references>.

[8] J. Gatheral. 2006. *The Volatility Surface: A Practitioner's Guide*. Wiley. <http://eu.wiley.com/WileyCDA/WileyTitle/productCd-0471792519.html>.

[9] J. Gatheral and A. Jacquier. 2011. Convergence of Heston to SVI. *Quantitative Finance* 11:8, 1129–1132. http://papers.ssrn.com/sol3/papers.cfm?abstract_id=1555251.

[10] J. Gatheral and A. Jacquier. 2013. Arbitrage-free SVI volatility surfaces, *Social Science Research Network*, March 17, p. 8. http://papers.ssrn.com/sol3/papers.cfm?abstract_id=2033323.

[11] G.E. Uhlenbeck and L.S. Ornstein. 1930. On the theory of Brownian motion *Phys. Rev* 36:823–841. http://prola.aps.org/abstract/PR/v36/i5/p823_1.

[12] S.L. Heston. 1993. A closed-form solution for options with stochastic volatility with applications to bond and currency options. *The Review of Financial Studies* 6:2, 327–343. <http://faculty.baruch.cuny.edu/lwu/890/Heston93.pdf>.

[13] N.E. Karoui. 2003. Couverture des risques dans les marches financiers, p. 92. Available at: <http://www.cmap.polytechnique.fr/elkaroui/masterfin034.pdf>.

[14] R. Lagnado and S. Osher. 2000. A technique for calibrating derivative security pricing models: Numerical solution of the inverse problem. *Risk* September. <http://www.risk.net/journal-of-computational-finance/technical-paper/2160492/a-technique-calibrating-derivative-security-pricing-models-numerical-solution-inverse>.

[15] C. Martini. 2009. Quasi-explicit calibration of Gatheral's SVI model, pp. 2–3. Available at: <http://www.zeliade.com/whitepapers/zwp-0005.pdf>.

[16] M. Planck. 1917. Sitzber. Preuss. Akad. Wiss., 324; M. Planck. 1958. *Physikalische Abhandlungen und Vortrage*, Vieweg, Braunschweig, p. 435.

[17] C. Rogers and M. Tehranchi. 2009. The implied volatility surface does not move by parallel shifts, pp. 7–10. Available at: <http://www.statslab.cam.ac.uk/chris/papers/iv.pdf>.

[18] P.J. Schonbucher. 1999. A market model for stochastic implied volatility, SFB 303 Working Paper No. B – 453, May. http://papers.ssrn.com/sol3/papers.cfm?abstract_id=182775.

[19] P. Tankov and N. Touzi. 2010. Calcul stochastique en finance, p. 146. Available at: http://www.math.jussieu.fr/tankov/Poly_MAP552.pdf.